Soil Evaporation

William P. Kustas

Hydrology and Remote Sensing Lab, U.S. Department of Agriculture, Agricultural Research Service (USDA-ARS), Beltsville, Maryland, U.S.A.

Nurit Agam

Blaustein Institutes for Desert Research, Ben-Gurion University of the Negev, Sede Boqer campus, ~~Beer-Sheva,~~ Israel

Abstract

Soil evaporation can significantly influence energy flux partitioning of partially vegetated surfaces, ultimately affecting plant transpiration. While important, quantification of soil evaporation, separately from canopy transpiration, is challenging. Techniques for measuring soil evaporation exist and continually improve. The large variability in soil water content requires that there be careful thought to the design of soil evaporation measurements in the field. Numerical models for simulating soil evaporation have been developed and are shown to be fairly robust. However, the required inputs for defining model parameters often limit their application. For many operational applications where detailed soils and ancillary weather data are unavailable or where daily evaporation values are only needed, some of the analytical models described may provide the necessary level of accuracy. Moreover, in the application of weather forecast and hydrologic models, the use of simplified approaches is necessitated by the computational requirements or the lack of adequate data or both for defining more complex numerical model inputs. For large area estimation, the use of remotely sensed soil moisture and surface temperature offer the greatest potential for operational applications.

INTRODUCTION

Soil evaporation not only determines partitioning of available energy between sensible and latent heat flux for bare soil surfaces but can also significantly influence energy flux partitioning of partially vegetated surfaces. This latter effect occurs via the impact of soil evaporation on the resulting surface soil moisture and temperature. These, in turn, strongly influence the microclimate in partially vegetated canopies, indirectly affecting plant transpiration.[1] Over a growing season, soil evaporation can be a significant fraction of total water loss for agricultural crops.[2] On a seasonal basis in semiarid and arid regions, soil evaporation can significantly alter the relative fraction of runoff to rainfall, which in turn has a major impact on the available water for plants.[3] In deserts, in spite of its small magnitude, soil evaporation can introduce significant errors in meteorological forecasting if neglected.[4]

The measurement of soil evaporation at field scale is typically obtained using standard micrometeorological techniques, namely Bowen ratio and eddy covariance methods. Traditionally, due to fetch and measurement requirements, under partial canopy cover conditions, these techniques are not able to partition the total evapotranspiration into its soil evaporation and plant transpiration components. Recently, a novel procedure for partitioning evapotranspiration through utilizing the measured high-frequency time series of carbon dioxide and water vapor concentrations has been developed and tested.[5] This approach relies upon the simple assumption that contributions to the time series of carbon dioxide and water vapor concentrations are derived from stomatal processes (i.e., photosynthesis and transpiration), and nonstomatal processes (i.e., respiration and direct evaporation) separately conform to flux-variance similarity. Vegetation water-use efficiency is the only parameter needed to perform the partitioning. Further work is needed to evaluate the utility of this technique with eddy covariance data collected over a variety of land cover and climate conditions.

Soil evaporation in partial canopy cover conditions varies spatially depending primarily on soil water distribution, canopy shading, and under-canopy wind patterns. These effects are magnified in row crops and under various irrigation techniques (e.g., drip irrigation). Soil evaporation can be measured using microlysimeters,[6] chambers,[7] time-domain reflectometers (TDRs),[8] a combination of microlysimetry and TDR,[9] micro-Bowen ratio systems,[3,10] or heat pulse probes.[11] Given the high spatial variability in the driving forces under partial canopy cover conditions, these point-based measurements are difficult to extrapolate to the field scale. Therefore, models have been developed to estimate the contribution of soil evaporation to the total evapotranspiration process.

Measurement methods are described, and models of varying degrees of complexity are reviewed, focusing primarily on relatively simple analytical models, some of which provide daily estimates and can be implemented operationally. The potential application of models using remote sensing data for large-scale estimation is also briefly discussed.

METHODOLOGIES

Measurement Methods

Microlysimeters

Microlysimeters have been widely used to measure evapo-ration from the soil surface of irrigated crops.[8,12,13] Typi-cally, an undisturbed soil sample (a representative vertical section of the soil profile) is inserted into a small cylinder open at the top. The microlysimeter is inserted back into the soil with its upper edge level with the soil surface and weighed either periodically or continuously. Changes in weight reflect an evaporative flux. To eliminate vertical heat conduction through the microlysimeter cylinder and minimize horizontal heat flux in the deeper layers of the sample, poly(vinyl chloride) (PVC) has been found to be the most suitable material. The microlysimeter's dimensions are typically a diameter of ~8 cm and a depth of 7–10 cm.[14–16] Theoretically, the microlysimeters provide absolute reference for soil evaporation, as long as their soil and the heat balance are similar to the surrounding area.

Chambers

Chambers are used to directly measure the flux of gases between the soil surface and the atmosphere by enclos-ing a volume and measuring all flux into and out of the volume.[17] Reviews of chamber designs and calculations of fluxes based on chamber methods can be found in Livingston and Hutchinson[18] and Hutchinson and Livingston.[19]

With infrared gas analyzers (IRGAs) becoming increas-ingly common, they are widely considered to be the method of choice today for chamber-based soil respiration and evaporation measurements.[20] Chambers can be used in either of two modes to calculate fluxes:[18] (1) in steady-state mode, the flux is calculated from the concentration difference between the air flowing at a known rate through the chamber inlet and outlet after the chamber headspace air has come to equilibrium concentration of carbon dioxide; (2) in the non-steady-state mode, the flux is calculated from the rate of increasing concentration in the chamber headspace of known volume shortly after the chamber is put over the soil.

In both modes, air is circulated between a small chamber that is placed on the soil and an IRGA. Typically, a soil chamber of ca. 1 L volume is placed on a PVC collar of about 80 cm^2 area. This collar is inserted about 2 cm into the soil and secured to prevent movement when the chamber is placed on it. When the chamber is placed on the collar, circulation of air between the chamber and the external IRGA is induced by a pump, and the water vapor concentration is measured.[21]

Soil water balance

Soil evaporation (*E*) can be extracted from the water balance equation, provided that all other components are known:

$$E = I + P - R + F - \Delta S \tag{1}$$

where *I* is irrigation, *P* is precipitation, *R* is runon or runoff, *F* is deep soil water flux (percolation), and ΔS is change in soil water storage. For an experimental field site, irrigation and precipitation can be easily monitored, and runoff and runon may be controlled to near-zero amounts by diking. Deep soil water flux errors can be reliably estimated in sev-eral ways, with the most important being the monitoring or measuring of the soil water content well below the root zone. The change in soil water storage can be determined fairly accurately with profile measurements of soil water content over multiple depths at the beginning and end of a defined time period.

There are many soil water content sensors, all of which work by measuring a surrogate property that is empirically or theoretically related to the soil water content. A recent comparative review by Evett et al.[22] concluded that soil water content is best determined using the neutron probe, gravimetric sampling, and conventional TDR[23] methods as compared to bore hole capacitance methods. Of the three optimal methods in the study, TDR is the only methodology capable of providing automated continuous measurements. However, other continuous measurement sensors such as frequency-domain reflectometers (FDRs),[24] and time-domain transmission (TDT)[25] sensors are also emerging as options for long-term installations, given appropriate calibration.

Micro-Bowen ratio systems

The Bowen ratio energy balance (BREB) approach is one of the simplest and most practical methods of estimating water vapor flux[10,26] and has thus been used extensively under a wide range of conditions providing robust esti-mates.[27] Use of the BREB concept[28] enables solving the energy balance equation by measuring simple gradients of air temperature and vapor pressure in the near-surface layer above the evaporating surface. The BREB equation is:

$$\lambda E = \frac{Rn - G}{1 + B_o} \tag{2}$$

in which λE is the latent heat flux, *Rn* is the net radiation, *G* is the soil heat flux, and B_0 the Bowen ratio, which is found from measurements of temperature and vapor pressure at two heights within the constant flux layer.[29] Assuming equal transfer coefficients for heat and vapor, the Bowen ratio is defined as:

$$B_o = \frac{H}{\lambda E} = \gamma \frac{\partial T}{\partial e} \tag{3}$$

where H is the sensible heat flux, γ is the psychrometric constant, T is the air temperature, and e is the water vapor pressure.

Application of the Bowen ratio concept to measure bare soil surface evaporation was suggested[3,10] by measuring temperature and vapor pressure close to the soil surface (e.g., at 1 and 6 cm). Compared to microlysimeters, the micro-Bowen ratio (MBR) system yielded good results over bare soil.[10] The potential of the MBR approach was demonstrated by successfully measuring soil evaporation within a maize field.[30] To date, test of the MBR is very limited, and further research is required to examine the performance of the technique under various environmental and agronomic conditions.

Heat pulse probes

A novel approach for measuring soil evaporation has been recently proposed, based on the soil sensible heat balance.[11,31] In this approach, a sensible heat balance is used to determine the amount of latent heat involved in the vaporization of soil water following Gardner and Hanks:[32]

$$LE = (H_0 - H_1) - \Delta S \tag{4}$$

where H_0 and H_1 are soil sensible heat fluxes at depths 0 and 1, respectively; ΔS is the change in soil sensible heat storage between depths 0 and 1; L is the latent heat of vaporization; and E is evaporation.

Typically, three-needle sensors like those described by Ren et al.[33] are used, which are spaced 6 mm apart, in parallel. Temperature is measured by all three needles, and the central needle also contains a resistance heater for producing a slight pulse of heat required for the heat pulse method. At a given time interval (2–4 hours), a heat pulse is executed, and the corresponding rise in temperature at the outer sensor needles is recorded. Soil volumetric heat capacity and thermal diffusivity are then determined from the heat input and temperature response following the procedures described by Knight and Kluitenberg[34] and Bristow et al.,[35] respectively. Having measurements of soil temperature, thermal conductivity, and volumetric heat, evaporation is estimated from Eq. 4.

Numerical Models

Numerous mechanistic/numerical models of heat and mass flows exist and are primarily based on the theory of Philip and de Vries.[36] However, they continue to be refined through improved parameterization of the moisture and heat transport through the soil profile.[37–39] Some of these mechanistic models have been used recently to explore the utility of bulk transfer approaches used in weather forecasting models[40] and in soil–vegetation–atmosphere models,[41] computing field to regional-scale fluxes. These bulk transport approaches are commonly called the "alpha" and "beta" methods defined by the following expressions

$$LE_s = \frac{\rho C_p}{\gamma}\left(\frac{ae_*(T_s) - e_A}{R_A}\right) \tag{5}$$

and

$$LE_s = \frac{\rho C_p}{\gamma}\beta\left(\frac{e_*(T_s) - e_A}{R_A}\right) \tag{6}$$

where ρ is the air density (~1kg/m³), C_p the heat capacity of air (~1000J/kg/K), γ the pyschrometric constant (~65Pa), $e_*(T_S)$ the saturated vapor pressure (Pa) at soil temperature T_S(K), e_A the vapor pressure (Pa) at some reference level in the atmosphere, and R_A is the resistance (s/m) to vapor transport from the surface usually defined from surface layer similarity theory.[42] For a, several different formulations exist[43,44] with one of the first relating a to the thermodynamic relationship for relative humidity in the soil pore space, h_R[45]

$$h_R = \exp\left(\frac{\psi g}{R_V T_S}\right) \tag{7}$$

where ψ is the soil matric potential (m), g the acceleration of gravity (9.8m/s²), and R_V the gas constant for water vapor (461.5J/kg/K). From Eq. 6, β can be defined as a ratio of aeodynamic and soil resistance to vapor transport from the soil layer to the surface, R_S, namely

$$\beta = \frac{R_A}{R_A + R_S} \tag{8}$$

Both modeling[44] and observational results[46,47] indicate that more reliable results are obtained using the beta method. In fact, Ye and Pielke[44] formulate an expression similar to Camillo and Gurney,[48] which combines Eqs. 5 and (6) and provides more reliable evaporation rates for a wider range of conditions,

$$LE_s = \frac{\rho C_p}{\gamma}\beta\left(\frac{ae_*(T_s) - e_A}{R_A}\right) \tag{9}$$

Unfortunately, there is no consensus concerning the depth in the soil profile to consider in defining the a and β terms. In particular, studies evaluating the soil resistance term R_S use a range of soil moisture depths: 0–1/2 cm,[48] 0–1 cm,[7] 0–2 cm,[39,46] and 0–5 cm.[39] The study conducted by Chanzy and Bruckler[38] appears to be one of the few studies that attempts to determine the most useful soil moisture depth for modeling soil evaporation by considering the penetration depth of passive microwave sensors of varying wavelengths. Using field data and numerical simulations with a mechanistic model, they find that the 0–5 cm depth, which can be provided by the L-band microwave frequency, appears to be the most adequate frequency for evaluating soil evaporation.

Besides the depth of the soil layer to consider, the equations relating soil moisture to R_S have ranged from linear to exponential (Table 1). Furthermore, observations and numerical models have shown that varies significantly throughout the day and that its magnitude is also affected by climatic conditions.[38,39]

These are not the only complicating factors that make the use of such a bulk resistance approach somewhat tenuous. From detailed observations of soil moisture changes and water movement, Jackson et al.,[49] found the soil water flux in the 0–9 cm depth to be very dynamic with fluxes at all depths continually changing in magnitude and sometimes direction over the course of a day. These phenomena observed by Jackson et al.[49] are owing in part to a process that occurs during soil drying where dry surface soil layer forms, significantly affecting the vapor transport through the profile.[50] Yamanaka et al.[51] recently developed and verified, using wind tunnel data, a simple energy balance model in which the soil moisture available for evaporation is defined using

the depth of the evaporating/drying front in the soil. This approach removes the ambiguity of defining the thickness of the soil layer and resulting moisture available for evaporation. However, the depth of the evaporating surface is not generally known *a priori*, nor can it be measured in field conditions; hence, this approach at present is limited to exploring the effects of evaporating front on R_S type formulations.

Analytical Models

To reduce the effect of temporal varying, R_S, Chanzy and Bruckler[38] developed a simple analytically based daily LE_S (E_D) model using simulations from their mechanistic model for different soil texture, moisture, and climatic conditions as quantified by potential evaporation (E_{PD}), as given by Penman.[52] The analytical daily model requires midday 0–5 cm soil moisture θ, daily potential evaporation, and daily average wind speed (U_D). The simple model has the following form

Table 1 Bulk soil resistance formulations, R_S, from previous studies

R_S formula (s/m)	Value of coefficients	Soil type	Depth (cm)	References
$R_S = a\left(\dfrac{\theta_S}{\theta}\right)^n + b$	$a = 3.5$	Loam[a]	0–1/2	[21]
	$b = 33.5$			
	$n = 2.3$			
$R_S = a(\theta_S - \theta) + b$	$a = 4{,}140$	Loam[b]	0–1/2	[48]
	$b = -805$			
$R_S = R_{SMIN} \exp[a(\theta_{MIN}-\theta)]$	$R_{SMIN} = 10$ s/m	Fine sandy loam	0–1	[7]
	$\theta_{MIN} = 15\%$			
	$a = 0.3563$			
$R_S = \dfrac{a\left(\theta_S - \theta\right)^n}{2.3 \times 10^{-4}\left(T_s / 273.16\right)^{1.75}}$	$a = 2.16 \times 10^2$	Loam	0–2	[46]
	$n = 10$			
	$\theta_s = 0.49$			
	$a = 8.32 \times 10^5$	Sand	0–2	[46]
	$n = 16.16$			
	$\theta_s = 0.392$			
$R_S = a\theta + b$	$a = -73{,}420 - -51{,}650$	Sand	0–2	[39]
	$b = 1{,}940 - 3{,}900$			
$R_S = exp\left(b - a\left(\dfrac{\theta}{\theta_S}\right)\right)$	$a = 4.3$	Silty clay loam[a]	0–5	[41]
	$b = 8.2$			
	$a = 5.9$	Gravelly sandy loam	0–5	[66]
	$b = 8.5$			

[a]Soil type for the data from Jackson et al.[49] was determined from texture-dependent soil hydraulic conductivity and matric potential equations of Clapp and Hornberger evaluated by Camillo and Gurney.[48]

[b]Soil type was determined from texture-dependent soil hydraulic conductivity and matric potential equations of Clapp and Hornberger evaluated by Sellers et al.[41]

$$\frac{E_D}{E_{PD}} = \left[\frac{exp\left(A\theta + B\right)}{1+exp\left(A\theta + B\right)} \right] C + \left(1 - C\right) \qquad (10a)$$

$$A = a + 5max\left(3 - E_{PD}, 0\right) \qquad (10b)$$

$$B = b - 5(-0.025b - 0.05)max(3 - E_{PD}, 0) + \alpha(U_D - 3) \quad (10c)$$

$$C = 0.90 - 0.05c(U_D - 3) \qquad (10d)$$

where the coefficients a, b, and c depend on soil texture (Table 2) and were derived from their detailed mechanistic model simulations for loam, silty clay loam, and clay soils.[38] In Fig. 1, a plot of Eq. 10a is given for two soil types, loam (Fig. 1A) and silty clay loam (Fig. 1B) under two climatic conditions, namely, a relatively low evaporative demand condition with $U_D = 1$ m/s and $E_{PD} = 2$ mm/d and high demand $U_D = 5$ m/s and $E_{PD} = 10$ mm/d. Notice the transition from $E_D/E_{PD} \sim 1$ to $E_D/E_{PD} < 1$ as a function of θ varies not only with the soil texture, but also with the evaporative demand. The simplicity of such a scheme outlined in Eq. 10 needs further testing for different soil textures and under a wider range of climatic conditions.

The ratio E_D/E_{PD} as a function of θ illustrated in Fig. 1 also depicts the effect of the two "drying stages" typically used to describe soil evaporation.[42] The "first stage" (S_1) of drying is under the condition where water is available in the near-surface soil to meet atmospheric demand, i.e., $E_D/E_{PD} \sim 1$. In the "second stage" (S_2) of drying, the water availability or θ falls below a certain threshold where the soil evaporation is no longer controlled by the evaporative demand, namely, $E_D/E_{PD} < 1$. Under S_2, several studies find that a simple formulation can be derived by assuming that the time change in θ is governed by desorption, namely, as isothermal diffusion with negligible gravity effects from a semi-infinite uniform medium. This leads to the rate of evaporation for S_2 being approximated by[42,53]

$$E_D = 0.5D_E t^{-1/2} \qquad (11)$$

where the desorptivity D_E (mm/d$^{1/2}$) is assumed to be a constant for a particular soil type and t is the time (in days) from the start of S_2. Although both numerical models and observations indicate that the soil evaporation is certainly a more complicated process than the simple analytical expression given by Eq. 11, a number of field studies[3,54–58] have shown that for S_2 conditions, reliable daily values can be obtained using Eq. 11. In many of these studies for determining D_E, the integral of Eq. 11 is used, which yields the cumulative evaporation as a function of $t^{1/2}$

$$\sum E_D = D_E \left(t - t_O\right)^{1/2} \qquad (12)$$

where t_O is the number of days where $E_D/E_{PD} \sim 1$ or is in S_1. In practice, observations of ΣE_D are plotted vs. $(t - t_O)^{1/2}$ and in many cases the choice of the starting point of S_2 is

**Table 2** Values of desorptivity, D_E, evaluated from various experimental sites

Desorptivity D_E (mm/d$^{1/2}$)	Soil type	References
4.96–4.30	Sand	[54]
5.08	Clay loam	[55]
4.04	Loam	[55]
3.5	Clay	[55]
~4 to ~8[a]	Loam[b]	[56]
5.8	Clay loam	[57]
4.95[c]	Silty clay loam[d]	[59]
2.11	Gravelly sandy loam	[3]

[a]The magnitude of D_E was found to have a seasonal dependency.
[b]Soil type was determined from texture-dependent soil hydraulic conductivity and matric potential equations of Clapp and Hornberger evaluated by Camillo and Gurney.[48]
[c]This value was evaluated for a vegetated surface.
[d]Soil type was determined from texture-dependent soil hydraulic conductivity and matric potential equations of Clapp and Hornberger evaluated by Sellers et al.[41]
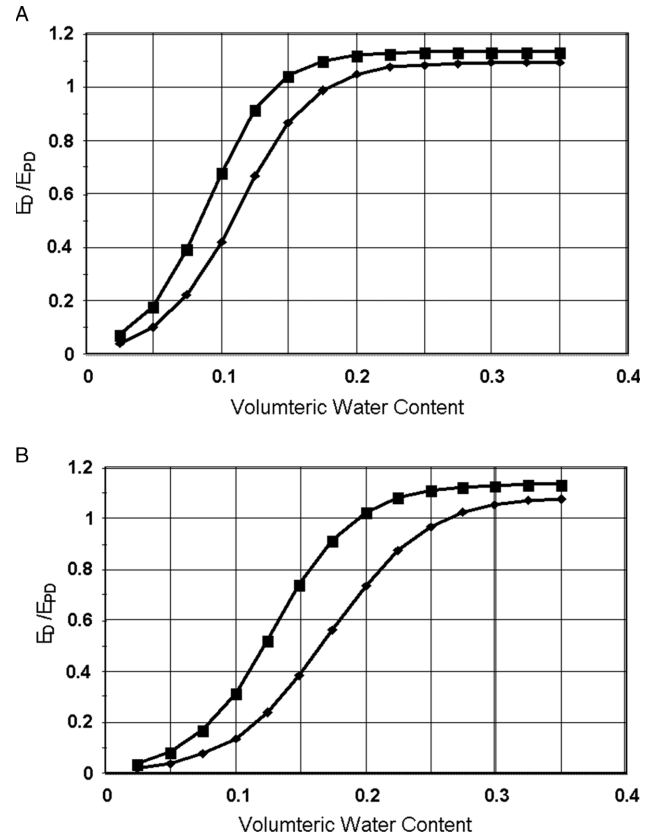
Fig. 1 A plot of E_D/E_{PD}, estimated using Eq. 10 from Chanzy and Bluckler[38] vs. volumetric water content for (**A**) loam and (**B**) silty clay loam soil under two evaporative demand conditions: $U_D = 1$ m/s and $E_{PD} = 2$ mm/d (squares) and $U_D = 5$ m/s and $E_{PD} = 10$ mm/d (diamonds).

$t_O \approx 0$ or immediately after the soil is saturated. As shown by Campbell and Norman,[58] the course of evaporation rate for three drying experiments (see Fig. 9.6 in Campbell and Norman[58]) indicates that for a loam soil, t_O depends on the evaporative demand or E_{PD} with $t_O \sim 2$ days when E_{PD} is high vs. $t_O \sim 5$ days when E_{PD} is low. On the other hand, for a sandy soil, there is almost an immediate change from S_1 to S_2 conditions with $t_O \approx 1$ day. As suggested by the analysis of Jackson et al.[56] and as stated more explicitly by Brutsaert and Chen,[59] the value of t_O can significantly influence the value computed for D_E. Jackson et al.[56] also show that for the same soil type, the value of D_E has a seasonal dependency (ranging from 4 to 8 mm/d$^{1/2}$) most likely related to the evaporative demand, which they correlate to daily average soil temperature (see Fig. 2 in Ref. 56). Values of D_E from the various studies are listed in Table 2. Brutsaert and Chen[59] modified Eq. 11 for deriving D_E by rewriting in terms of a "time-shifted" variable $T = t - t_O$ and expressing it in the form

$$E_D^{-2} = \left(\frac{2}{D_E}\right)^2 T \tag{13}$$

where D_E and t_O will come from the slope and intercept (see Fig. 1 in Brutsaert and Chen[59]). It follows that ΣE_D under S_2 will start at $T = T_O$ and not at $T = 0$, so that Eq. 12 is rewritten as

$$\sum E_D = D_E \left(T^{1/2} - T_O^{1/2}\right) \tag{14}$$

They evaluated the effect on the derived D_E using this technique with the data from Black et al.[54] The value of D_E using Eqs. 13 and 14 was estimated to be approximately 3.3 mm/d$^{1/2}$, which is smaller than D_E values reported by Black et al.,[54] namely, 4.3–5 mm/d$^{1/2}$. However, Brutsaert and Chen[59] show that this technique yields a better linear fit to the data points that were actually under S_2 conditions.

Equations 13 and 14 were used with the September 1973 data set from Jackson et al.[56] and compared to using Eq. 12 with $t_O = 0$. The plot of Eq. 12 with the regression line in Fig. 2 yields $D_E \sim 10$ mm/d$^{1/2}$, which is significantly larger than any previous estimates (Table 2). Moreover, it is obvious from the figure that Eq. 12 should not be applied with $t_O = 0$, as this relationship is not linear over the whole drying processes. With Eq. 13, applied to the data, t_O is estimated to be approximately 4.3 days, and thus a linear relationship should start at the shifted time scale $T = t - 4.3$; this means ΣE_D should start on day 5 or $T_O \approx 5 - 4.3$ (Fig. 3A). With Eq. 14, a more realistic $D_E \approx 4.6$ mm/d$^{1/2}$ is estimated for the linear portion of daily evaporation following the S_2 condition (Fig. 3B).

While this approach is relatively easy to implement operationally, D_E will likely depend on climatic factors as well as soil textural properties. However, it might be feasible
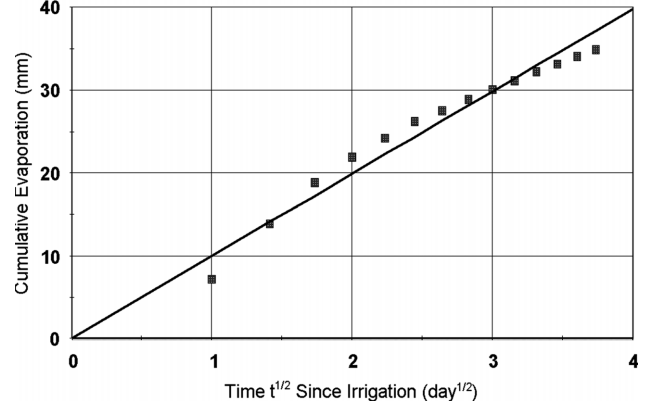
Fig. 2 The desorptivity D_E (mm/d$^{1/2}$) estimated from a least squares linear fit to the data from Jackson et al.[56] assuming $t_O = 0$ (i.e., stage-two drying occurs immediately after irrigation/precipitation).
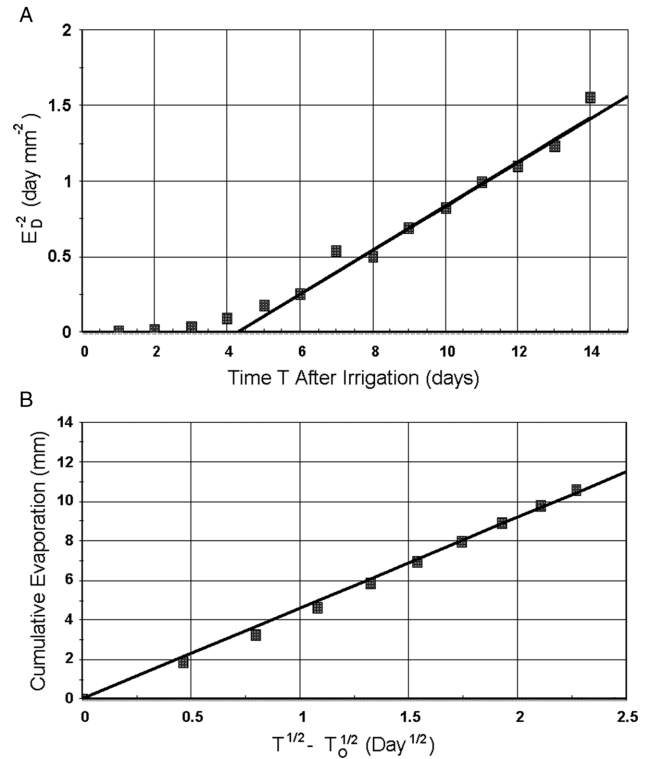
Fig. 3 Estimation of (**A**) D_E and t_O with the data from Fig. 2 using Eq. 13 from Brutsaert and Chen[59] and (**B**) the resulting cumulative evaporation ΣE_D curve under second stage drying using Eq. 14.

to describe the main climate/seasonal effect on D_E from soil temperature observations.[56] These might come from weather station observations or possibly from multitemporal remote sensing observations of surface temperature.

The difficulty in developing a formulation for R_S, which correctly describes the water vapor transfer process in the soil, was recognized much earlier by Fuchs and Tanner[60]

and Tanner and Fuchs.[61] They proposed a combination method instead that involves atmospheric surface layer observations and remotely sensed surface temperature, T_{RS}. Starting with the energy balance equation

$$R_N = H + G + LE \tag{15}$$

where R_N is the net radiation, H the sensible heat flux, and G the soil heat flux all in W/m², and assuming the resistance to heat and water vapor transfer are similar yielding,

$$H = \rho C_P \left(\frac{T_{RS} - T_A}{R_A} \right) \tag{16}$$

$$LE = \frac{\rho C_P}{\gamma} \left(\frac{e_{RS} - e_A}{R_A} \right) \tag{17}$$

an equation of the following form can be derived

$$LE = \left(\frac{\gamma + \Delta}{\Delta} \right) LE_P - \frac{\rho C_P}{\Delta} \left(\frac{e_*(T_{RS}) - e_A}{R_A} \right) \tag{18}$$

where

$$LE_P = \rho C_P \left(\frac{e_*(T_A) - e_A}{R_A (\Delta + \gamma)} \right) + \Delta \left(\frac{R_N - G}{\Delta + \gamma} \right) \tag{19}$$

The difference $e_*(T_A) - e_A$ is commonly called the saturation vapor pressure deficit, and the value of soil surface vapor pressure e_{RS} is equal to $h_{RS} e_*(T_{RS})$ where h_{RS} is the soil surface relative humidity. Substituting Eq. 19 into Eq. 18 yields

$$LE = R_N - G - \frac{\rho C_P}{\Delta} \left(\frac{e_*(T_{RS}) - e_*(T_A)}{R_A} \right) \tag{20}$$

This equation has the advantage over the above bulk resistance formulations using R_S in that there are no assumptions made concerning the saturation deficit at or near the soil surface or how to define h_{RS}. Instead, this effect is accounted for by T_{RS} because as the soil dries, T_{RS} increases and hence $e_*(T_{RS})$, which generally results in the last term on the right-hand side of Eq. 20 to increase, thus causing LE to decrease. In a related approach,[62] the magnitude of LE is simply computed as a residual in the energy balance equation, Eq. 19, namely

$$LE = R_N - G - \rho C_P \left(\frac{T_{RS} - T_A}{R_A} \right) \tag{21}$$

Particularly crucial in the application of either Eq. 20 or 21 is a reliable estimate of R_A and T_{RS}. Issues involved in correcting radiometric temperature observations for surface emissivity, viewing angle effects, and other factors are summarized in Norman and Becker.[63] The aerodynamic

resistance R_A is typically expressed in terms of Monin–Obukhov similarity theory[42]

$$R_A = \frac{\left\{ \ln \left[\frac{z - d_O}{z_{OM}} \right] - \psi_M \right\} \left\{ \ln \left[\frac{z - d_O}{z_{OS}} \right] - \psi_S \right\}}{k^2 U} \tag{22}$$

where z is the observation height in the surface layer (typically 2–10 m), d_O the displacement height, z_{OM} the momentum roughness length, z_{OS} the roughness length for scalars (i.e., heat and water vapor), k (~0.4) von Karman's constant, ψ_M the stability correction function for momentum, and ψ_S the stability correction function for scalars. Both d_O and z_{OM} are dependent on the height and density of the roughness obstacles and can be considered a constant for a given surface, while the magnitude of z_{OS} can vary for a given bare soil surface as it is also a function of the surface friction velocity.[42] Experimental evidence suggests that existing theory with possible modification to some of the "constants" can still be used to determine z_{OS} providing acceptable estimates of H for bare soil surfaces. However, application of Eq. 21 in partial canopy cover conditions has not been successful in general because z_{OS} is not well defined in Eq. 22, exhibiting large scatter with the existing theory.[64]

For this reason, estimating soil evaporation from partially vegetated surfaces using T_{RS} invariably has to involve "two-source" approaches whereby the energy exchanges from the soil and vegetated components are explicitly treated.[65] Similarly, when using remotely sensed soil moisture for vegetated surfaces, a two-source modeling framework needs to be applied.[66] In these two-source approaches, there is the added complication of determining aerodynamic resistances between soil and vegetated surfaces and the canopy air space. Schematically, the resistance network and corresponding flux components for two-source models is shown in Fig. 4. An advantage with the two-source formulation of Norman et al.[65] is that R_S is not actually needed for computing LE_S as it is solved as a residual. Nevertheless, the formulations in such parameterizations that are used (such as the aerodynamic resistance formulations) are likely to strongly influence LE_S values.[1] Yet this two-source formulation is found to be fairly robust in separating soil and canopy contributions to evapotranspiration.[67]

CONCLUSIONS

Techniques for measuring soil evaporation, separately from plant transpiration, exist and continually improve. Given the high variability in soil water content often exhibited in the field, the exact position of the instrumentation may have a large effect on the measurement. This is magnified in row crops, where the variability is structured, rather than random. In row crops, soil evaporation is not only dependent
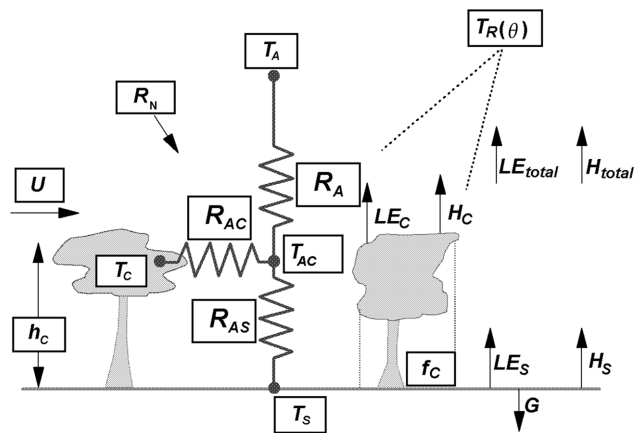
Fig. 4 A schematic diagram illustrating the resistance network for the two-source approach where the subscript c refers to the vegetated canopy and s refers to the soil surface. The symbol $T_R(\theta)$ refers to a radiometric temperature observation at a viewing angle θ, T_{AC} is the model-derived within-canopy air space temperature, h_C is the canopy height, f_C is the fractional vegetation/canopy cover, and R_{AC} and R_{AS} are the aerodynamic resistances to sensible heat flux from the canopy and soil surface, respectively. The main meteorological inputs required for the model are also illustrated, namely wind speed, U, air temperature, T_A, and the net radiation, R_N.

Source: Adapted from Norman et al.[65]

on the soil properties, but also local climatic conditions, and the timing of irrigation/precipitation. Under low-to-moderate wind speed conditions (~1 to 4 m s^{-1}), row orientation relative to the wind direction also affects the amount of soil evaporation.[68] This large variability requires that there be careful thought to the design of soil evaporation measurements in the field. The methodology proposed by Scanlon and Kustas[5] using eddy covariance measurements suffers less from the sampling issue but requires *a priori* knowledge of the vegetation water-use efficiency, which will vary with vegetation type and condition.

For many landscapes having partial vegetative cover, the contribution of soil evaporation to the total evapotranspiration flux cannot be ignored, particularly with regard to the influence of surface soil moisture and temperature on the microclimate in the canopy air space (Fig. 4). Numerical models for simulating soil evaporation have been developed and are shown to be fairly robust. However, the required inputs for defining model parameters often limit their application to field sites having detailed soil profile information and that are well instrumented with ancillary weather data.

For many operational applications where detailed soil and ancillary weather data are unavailable or where daily evaporation values are only needed, some of the analytical models described may provide the necessary level of accuracy. Moreover, in the application of weather forecast and hydrologic models, the use of simplified approaches is necessitated by the computational requirements or the lack of adequate data or both for defining more complex numerical model parameters and variables.

For large area estimation, the use of remotely sensed soil moisture and surface temperature offer the greatest potential for operational applications. The development of modeling schemes that can incorporate this remote sensing information and readily apply it on a regional scale basis have been proposed and show promise.[66,69–71]

REFERENCES

1. Kustas, W.P.; Norman, J.M. Evaluation of soil and vegetation heat flux predictions using a simple two-source model with radiometric temperatures for partial canopy cover. Agric. Forest Meteorol. **1999**, *94*, 13–25.
2. Tanner, C.B.; Jury, W.A. Estimating evaporation and transpiration from a row crop during incomplete cover. Agron. J. **1976**, *68*, 239–242.
3. Wallace, J.S.; Holwill, C.J. Soil evaporation from tiger-bush in south-west Niger. J. Hydrol. **1997**, *188–189*, 426–442.
4. Agam, N.; Berliner, P. R.; Zangvil, A.; Ben-Dor, E. Soil water evaporation during the dry season in an arid zone. *J. Geophys. Res. Atmos.* **2004**, *109*, D16103, doi:16110.11029/12004JD004802.
5. Scanlon, T.M.; Kustas, W.P. Partitioning carbon dioxide and water vapor fluxes using correlation analysis. Agric. Forest Meteorol. **2010**, *150*, 89–99.
6. Allen, S.J. Measurement and estimation of evaporation from soil under sparse barley crops in northern Syria. Agric. Forest Meteorol. **1990**, *49*, 291–309.
7. Van de griend, A.A.; Owe, M. Bare soil surface resistance to evaporation by vapor diffusion under semiarid conditions. Water Resour. Res. **1994**, *30*, 181–188.
8. Plauborg, F. Evaporation from bare soil in a temperate humid climate - Measurement using micro-lysimeters and time domain reflectometry. Agric. Forest Meteorol. **1995**, *76*, 1–17.
9. Baker, J.M.; Spaans, E.J. Measuring water exchange between soil and atmosphere with TDR-Microlysimetry. Soil Sci. **1994**, *158*, 22–30.
10. Ashktorab, H.; Pruitt, W.O.; Pawu, K.T.; George, W.V. Energy-balance determinations close to the soil surface using a micro-Bowen ratio system. Agric. Forest Meteorol. **1989**, *46*, 259–274.
11. Heitman, J.L.; Horton, R.; Sauer, T.J.; Desutter, T.M. Sensible heat observations reveal soil-water evaporation dynamics. J. Hydrometeorol. **2008a**, *9*, 165–171.
12. Shawcroft, R.W.; Gardner, H.R. Direct evaporation from soil under a row crop canopy. Agric. Meteorol. **1983**, *28*, 229–238.
13. Lascano, R.J.; Van bavel, C.H.M. Simulation and measurement of evaporation from a bare soil. Soil Sci. Soc. Am. J. **1986**, *50*, 1127–1133.
14. Boast, C.W.; Robertson, T.M. A "micro-lysimeter" method for determining evaporation from bare-soil: description and laboratory evaluation. Soil Sci. Soc. Am. J. **1982**, *46*, 689–696.
15. Walker, G.K. Measurement of evaporation from soil beneath crop canopies. Can. J. Soil Sci. **1983**, *63*, 137–141.

16. Evett, S.R.; Warrick, A.W.; Matthias, A.D. Wall material and capping effects on microlysimeter temperatures and evaporation. Soil Sci. Soc. Am. J. **1995**, *59*, 329–336.

17. Denmead, O.T.; Dunin, F.X.; Wong, S.C.; Greenwood, E.A.N. Measuring water use efficiency of Eucalyptus trees with chambers and micrometeorological techniques. J. Hydrol. **1993**, *150*, 649–664.

18. Livingston, G.P.; Hutchinson, G.L. Enclosure-based measurement of trace gas exchange: Applications and sources of error. In *Biogenic Trace Gases: Measuring Emissions from Soil and Water*; Matson, P.A., Harriss, R.C., Eds.; Blackwell Scientific Publications: Oxford, 1995; pp. 14–51.

19. Hutchinson, G.L.; Livingston, G.P. Gas flux. In *Methods of Soil Analysis: Part 1, Physical Methods*; Dane, J.H., Topp, G.C., Eds.; Soil Science Society of America: Madison, WI: 2002.

20. Davidson, E.A.; Savage, K.; Verchot, L.V.; Navarro, R. Minimizing artifacts and biases in chamber-based measurements of soil respiration. Agric. Forest Meteorol. **2002**, *113*, 21–37.

21. Norman, J.M.; Kucharik, C.J.; Gower, S.T.; Baldocchi, D.D.; Crill, P.M.; Rayment, M.; Savage, K.; Striegl, R.G. A comparison of six methods for measuring soil-surface carbon dioxide fluxes. J. Geophys. Res.-Atmospheres **1997**, *102*, 28771–28777.

22. Evett, S.R.; Schwartz, R.C.; Casanova, J.J.; Heng, L.K. Soil water sensing for water balance, ET and WUE. Agric. Water Manag. **2012**, *104*, 1–9.

23. Topp, G.C.; Davis, H.L.; Annan, A.P. Electromagnetic determination of soil water content: measurements in coaxial transmission lines. Water Resour. Res. **1980**, *16*, 574–582.

24. Logsdon, S.D.; Green, T.R.; Seyfried, M.S.; Evett, S.R.; Bonta, J. Hydra Probe and Twelve-Wire Probe comparisoins in fluids and soil cores. Soil Sci. Soc.Am. J. **2010**, *74*, 5–12.

25. Miralles-crespo, J.; Van lersel, M.W. A calibrated time domain transmissometry soil moisture sensor can be used for precise automated irrigation of container-grown plants. HortScience **2011**, *46*, 889–894.

26. Allen, R.G.; Pereira, L.S.; Howell, T.A.; Jensen, M.E. Evapotranspiration information reporting: I. Factors governing measurement accuracy. Agric. Water Manag. **2011**, *98*, 899–920.

27. Farahani, H.J.; Howell, T.A.; Shuttleworth, W.J.; Bausch, W.C. Evapotranspiration: Progress in measurement and modeling in agriculture. Trans. Am. Soc. Agric. Biol. Engineers **2007**, *50*, 1627–1638.

28. Bowen, I.S. The ratio of heat losses by conduction and by evaporation from any water surface. Phys. Rev. **1926**, *27*, 779–787.

29. Monteith, J.L.; Unsworth, M.H. *Principles of Environmental Physics*, 3rd ed.; Elsevier/Academic Press: 2008.

30. Zeggaf, A.T.; Takeuchi, S.; Dehghanisanij, H.; Anyoji, H.; Yano, T. A Bowen ratio technique for partitioning energy fluxes between maize transpiration and soil surface evaporation. Agronomy J. **2008**, *100*, 988–996.

31. Heitman, J.L.; Xiao, X.; Horton, R.; Sauer, T.J. Sensible heat measurements indicating depth and magnitude of subsurface soil water evaporation. Water Resour. Res. **2008b**, *44*.

32. Gardner, H.R.; Hanks, R.J. Evaluation of the evaporation zone in soil by measurement of heat flux. Soil Sci. Soc. Am. Proc. **1966**, *32*, 326–328.

33. Ren, T.S.; Ochsner, T.E.; Horton, R. Development of thermo-time domain reflectometry for vadose zone measurements. Vadose Zone J. **2003**, *2*, 544–551.

34. Knight, J.H.; Kluitenberg, G.J. Simplified computational approach for dual-probe heat-pulse method. Soil Sci. Soc. Am. Journal. *68*, 447–449.

35. Bristow, K.L.; Kluitenberg, G.J.; Horton, R. Measurement of soil thermal-properties with a dual-probe heat-pulse technique. Soil Sci. Soc. Am. J. **1994**, *58*, 1288–1294.

36. Philip, J.R.; De vries, D.A. Moisture movement in porous materials under temperature gradients. Trans. Am. Geophys. Union **1957**, *38* (2), 222–232.

37. Camillo, P.J.; Gurney, R.J.; Schmugge, T.J. A soil and atmospheric boundary layer model for evapotranspiration and soil moisture studies. Water Resour. Res. **1983**, *19*, 371–380.

38. Chanzy, A.; Bruckler, L. Significance of soil surface moisture with respect to daily bare soil evaporation. Water Resour. Res. **1993**, *29*, 1113–1125.

39. Daamen, C.C.; Simmonds, L.P. Measurement of evaporation from bare soil and its estimation using surface resistance. Water Resour. Res. **1996**, *32*, 1393–1402.

40. Noilhan, J.; Planton, S. A simple parameterization of land surface processes for meteorological models. Mon. Weather Rev. **1989**, *117*, 536–549.

41. Sellers, P.J.; Heiser, M.D.; Hall, F.G. Relations between surface conductance and spectral vegetation indices at intermediate (100m^2 to 15km^2) length scales. J. Geophys. Res. **1992**, *97*, 19033–19059.

42. Brutsaert, W. *Evaporation into the Atmosphere: Theory, History and Applications*; D. Reidel Publishing Co.: Boston, 1982.

43. Mahfouf, J.F.; Noilhan, J. Comparative study of various formulations of evaporation from bare soil using in situ data. J. Appl. Meteorol. **1991**, *30*, 1354–1365.

44. Ye, Z.; Pielke, R.A. Atmospheric parameterization of evaporation from non-plant-covered surfaces. J. Appl. Meteorol. **1993**, *32*, 1248–1258.

45. Philip, J.R. 1957, Evaporation, and moisture and heat fields in the soil. Journal of Meteorology. *14*, 354–366.

46. Kondo, J.; Saigusa, N.; Sato, T. A parameterization of evaporation from bare soil surfaces. J. Appl. Meteorol. **1990**, *29*, 385–389.

47. Cahill, A.T.; Parlange, M.B.; Jackson, T.J.; O'Neill, P.; Schmugge, T.J. Evaporation from nonvegetated surfaces: Surface aridity methods and passive microwave remote sensing. J. Appl. Meteorol. **1999**, *38*.

48. Camillo, P.J.; Gurney, R.J. A resistance parameter for bare-soil evaporation models. Soil Sci. **1986**, *141*, 95–104.

49. Jackson, R.D.; Kimball, B.A.; Reginato, R.J.; Nakayama, F.S. Diurnal soil water evaporation: Time-depth-flux patterns. Soil Sci. Soc. Am. Proc. **1973**, *37*, 505–509.

50. Hillel, D. *Applications of Soil Physics*; Academic Press: San Diego, 1980.

51. Yamanaka, T.; Takeda, A.; Sugita, F. A modified surface-resistance approach for representing bare-soil evaporation: Wind tunnel experiments under various atmospheric conditions. Water Resour. Res. **1997**, *33*, 2117–2128.

52. Penman, H.L. Natural evaporation from open water, bare soil and grass, Proc. R. Soc. Lond. **1948**, *A193*, 120–146.

53. Gardner, W.R. Solution of the flow equation for the drying of soils and other porous media. Soil Sci. Soc. Am. Proc. **1959**, *23*, 183–187.

54. Black, R.A.; Gardner, W.R.; Thurtell, G.W. The prediction of evaporation, drainage, and soil water storage for a bare soil. Soil Sci. Soc. Am. Proc. **1969**, *33*, 655–660.

55. Ritchie, J.T. Model for predicting evaporation from a row crop with incomplete cover. Water Resour. Res. **1972**, *8*, 1204–1213.

56. Jackson, R.D.; Idso, S.B.; Reginato, R.J. Calculation of evaporation rates during the transition from energy-limiting to soil-limiting phases using albedo data. Water Resour. Res. **1976**, *12*, 23–26.

57. Parlange, M.B.; Katul, G.G.; Cuenca, R.H.; Kavvas, M.L.; Nielsen, D.R.; Mata, M. Physical basis for a time series model of soil water content. Water Resour. Res. **1992**, *28*, 2437–2446.

58. Campbell, G.S.; Norman, J.M. An Introduction To Environmental Biophysics; Springer-Verlag: New York, 1998.

59. Brutsaert, W.; Chen, D. Desorption and the two stages of drying of natural tallgrass prairie. Water Resour. Res. **1995**, *31*, 1305–1313.

60. Fuchs, M.; Tanner, C.B. Evaporation from a drying soil. J. Appl. Meteorol. **1967**, *6*, 852–857.

61. Tanner, C.B.; Fuchs, M. Evaporation from unsaturated surfaces: a generalized combination method. J. Geophys. Res. **1968**, *73*, 1299–1304.

62. Jackson, R.D.; Reginato, R.J.; Idso, S.B. Wheat canopy temperature: A practical tool for evaluating water requirements. Water Resour. Res. **1977**, *13*, 651–656.

63. Norman, J.M.; Becker, F. Terminology in thermal infrared remote sensing of natural surfaces. Agric. Forest Meteorol. **1995**, *77*, 153–166.

64. Verhoef, A.; De bruin, H.A.R.; Van den hurk, B.J.J.M. Some practical notes on the parameter kB-1 for sparse vegetation. J. Appl. Meteorol. **1997**, *36*, 560–572.

65. Norman, J.M.; Kustas, W.P.; Humes, K.S. A two-source approach for estimating soil and vegetation energy fluxes in observations of directional radiometric surface temperature. Agric. Forest Meteorol. **1995**, *77*, 263–293.

66. Kustas, W.P.; Zhan, X.; Schmugge, T.J. Combining Optical and Microwave Remote Sensing for Mapping Energy Fluxes in a Semiarid Watershed. Remote Sensing Environ. **1998**, *64*, 116–131.

67. Kustas, W.P.; Anderson, M.C. Advances in Thermal Infrared Remote Sensing for Land Surface Modeling. Agric. Forest Meteorol. **2009** (in press).

68. Agam, N.; Evett, S.R.; Tolk, J.A.; Kustas, W.P.; Colaizzi, P.D.; Alfieri, J.G.; Mckee, L.G.; Copeland, K.S.; Howell, T.A.; Chávez, J.L. Evaporative loss from irrigated interrows in a highly advective semi-arid agricultural area. Adv. Water Resour. **2012**, http://dx.doi.org/10.1016/j.advwatres.2012.07.010

69. Mecikalski, J.R.; Diak, G.R.; Anderson, M.C.; Norman, J.M. Estimating fluxes on continental scales using remotely sensed data in an atmospheric-land exchange model. J. Appl. Meteorol. **1999**, *38*, 1352–1369.

70. Kustas, W.P.; Jackson, T.J.; French, A.N.; Macpherson, J.I. Verification of patch- and regional-scale energy balance estimates derived from microwave and optical remote sensing during SGP97. J. Hydrometeorol. **2001**, *2*, 254–273.

71. Anderson, M.C.; Kustas, W.P.; Norman, J.M.; Hain, C.R.; Mecikalski, J.R.; Schultz, L.; Gonzalez-dugo, M.P.; Cammalleri, C.; D'urso, G.; Pimstein, A.; Gao, F. Mapping daily evapotranspiration at field to continental scales using geostationary and polar orbiting satellite imagery. Hydrol. Earth Syst. Sci. **2011**, *15*, 223–239.